Vol.7 No.2 Journal of Computational Mathematics April 1989

COMPUTATION OF A 3–D VISCOUS COMPRESSIBLE NAVIER–STOKES EQUATION FOR SPINNING SHELLS AT MODERATE ANGLES OF ATTACK AND FOR LONG L/D FINNED PROJECTILES

HUANG AI–XIANG
(*Xi'an Jiaotong University, China*)

1. Introduction

The accurate prediction of projectile aerodynamics is of significant importance in the early stage of projectile design.

In recent years, considerable research effort has been focused on the development of modern predictive capabilities for determining projectile aerodynamics, and numerical methods have recently been developed using the 3–D viscous compressible Navier–Stokes computational technique to compute the flow over slender bodies of revolution at transonic or supersonic speeds.

Significant improvement has been made by the author in this paper to make this technique applicable to more complicated flow, by employing finite element methods, the splitting technique of nonlinear operators and the conjugate gradient method for nonlinear subproblems, reduction of an exterior problem into a boundary integral equation, and the domain decomposition method. Applications of the technique are made to a standard shell configuration to establish a benchmark for the code.

2. The Compressible Navier–Stokes Equation in a 3–D Noninertial Coordinate System

We use noninertial curvilinear coordinates $\{x^i\}$ in a rotating reference frame with angular velocity ω. The coordinate axis $z = x^3$ is fixed.

The constitution equation and the dissipation function are given by

$$\tau_{ij} = -pg_{ij} + t_{ij}, \tag{2.1}$$

$$t_{ij}(w) = -\frac{2}{3}\mu_v g_{ij} \text{ div } w + 2\mu_v e_{ij}(w) \tag{2.2}$$

and

$$f_e = -\frac{2}{3}\mu_v(\text{ div } w)^2 + 2\mu_v e^{ij}(w)e_{ij}(w). \tag{2.3}$$

The equations of continuity, momentum and energy for the gas-dynamics in coordinate system $\{x^i\}$ are given by

$$\begin{aligned} &\frac{\partial \rho}{\partial t} + \nabla_i(\rho w^i) = 0, \\ &\rho(\frac{\partial w^i}{\partial t} + w^j\nabla_j w^i + 2\varepsilon^{ijk}\omega_j w_k - (\omega)^2 r^i) = \nabla_j r^{ij} + f^i, \\ &\rho C_v(\frac{\partial T}{\partial t} + w^j\nabla_j T) + p\nabla_j w^j = \text{ div } (k\nabla T) + f_e + h, \\ &p = (r-1)C_v RT \end{aligned} \tag{2.4}$$

where h is heat source per unit volume.

The turbulence models used here are called eddy-viscosity models and are presented for the Navier-Stokes equation (1.1) by expressing μ_v and μ_e in terms of an eddy-viscosity function μ_T, *i.e.*,

$$\mu_v = \mu + \mu_T, \quad \mu_e = r(\frac{\mu}{p_r} + \frac{\mu_T}{p_{r_T}}), \quad r = C_p/C_v, \quad k = C_v\mu_e \tag{2.5}$$

where μ is the molecular viscosity coefficient, μ_T the turbulent viscosity coefficient, μ_e the conductivity, k the conductive coefficient, p_r the Prandtl number, and p_{rT} the turbulent Prandtl number.

The two-equation model employs two additional PDE for variables that are used to define the eddy-viscosity function (K–ε equations). The K–ε equations are given by

$$\text{div } (D_1 \text{ grad } K) = f_1, \quad \text{div } (D_2 \text{ grad } \varepsilon) = f_2$$

where f_1, f_2 are turbulent sources, and the turbulent viscosity is determined by

$$\mu_T = C_v\rho k^2/\varepsilon.$$

We now discuss the boundary conditions. The exterior domain Ω' is decomposed into two regions Ω_s and Ω_2 by a smooth artificial boundary Γ_2. The boundaries of Ω_s consist of the body surface Γ_s and artificial boundary Γ_2. The domain Ω_2 is unbounded. Then,

$$w|_{\Gamma_s} = 0, \quad T|_{\Gamma_s} = 0, \quad w|_{\Gamma_2} = w_\infty, \quad T|_{\Gamma_2} = T_\infty.$$

However, we have another way to treat the artificial boundary condition. In fact, for a far field from body Ω_s, the flow can be assumed to be a potential and imcompressible, nonviscous flow. Let us consider the momentum equation. Because

$$w|_{\Gamma_s} = 0 \text{ and } \tau^{ij}(w)n_j|_{\Gamma_2} = (-pg^{ij}n_j + 2\mu_v e^{ij}(w)n_j)|_{\Gamma_2} = -pn^i$$

we have

$$(w^j\nabla_j w^i, v_j) + 2(\varepsilon^{ijk}\omega_j w_k, v_j) + (\tau^{ij}(w), e_{ij}(w)) + \iint_{\Gamma_2}\frac{1}{\varepsilon}\ \text{div}\ (\rho w)vnds = (f_1, v)$$

where the penalty method is employed. On the other hand, setting $w = w_\infty + \mu$, we obtain the equation of μ.

3. Variational Formulation and Finite Element Approximation

Setting

$$(a,b) = \iiint_\Omega abdv, \quad dv = \sqrt{g}dx^1dx^2dx^3,$$

we have the variational formulation

$$\frac{d}{dt}(\rho,\rho^*) - (\rho w, \nabla\rho^*) + \iint_{\Gamma_2}\rho\rho^* wnds, \quad \forall\rho^*\in H^1(\Omega), \tag{3.1}$$

$$\begin{aligned}&\frac{d}{dt}(\rho w, w^*) - (\rho w^i w^j, e_{ij}(w^*)) + 2(\varepsilon^{ijk}\omega_j w_k\rho, w_i^*)\\ &-\frac{2}{3}(\mu_v\ \text{div}\ w,\ \text{div}\ w^*) - 2(\mu_v e^{ij}(w), e_{ij}(w^*))\\ &= (r-1)C_v(\rho T,\ \text{div}\ w^*) + ((\omega)^2\rho r^i, w_i^*) + (f, w^*)\\ &+\int_{\Gamma_2}(\tau^{ij} - \rho w^i w^j)n_j w_i^* ds, \quad \forall w^*\in h^1(\Omega),\end{aligned} \tag{3.2}$$

$$\begin{aligned}&\frac{d}{dt}(C_v\rho T, T^*) + (k\nabla T, \nabla T^*) - (C_v T\rho w, \nabla T^*) + ((r-1)C_v\rho T\ \text{div}\ w, T^*)\\ &= (f_e, T^*) + (h, T^*) + \iint_{\Gamma_2}(k\frac{\partial T}{\partial n}T^* - TT^*\rho wn)ds, \quad \forall T^*\in H^1(\Omega).\end{aligned} \tag{3.3}$$

Suppose $M_h\subset H^1(\Omega), (S_h)^3\subset H^1(\Omega)$ are finite element subspaces, and

$$\Phi^T = \{\Phi_1,\Phi_2,\ldots,\Phi_n\}, \quad \Psi^T = \{\Psi_1,\Psi_2,\cdots,\Psi_m\}$$

are base functions of s_h, M_h respectively. For $w_h^i\in S_h, T_h\in M_h, \rho_h\in M_h$, we have

$$w_n^i = \Phi^T w^i, \quad T_h = \Psi^T T, \quad \rho_h = \Psi^T R. \tag{3.4}$$

By use of (3.4), the finite element equations can be obtained from (3.1)–(3.3) as

$$M_0\frac{d\rho_h}{dt} = E(\rho_h)W_h, \tag{3.5}$$

$$M(\rho_h)\frac{dW_h}{dt} + K(\mu_v)W_h + N(\rho_h, W_h)W_h + F(\rho_h, T_h) = 0, \tag{3.6}$$

$$M_1(\rho_h)\frac{dT_h}{dt} + LT_h + N_0(\rho_h, W_h)T_h = F_0(W_h) \tag{3.7}$$

where $M_0, M(\rho_h), M_1(\rho_h)$ are mass matrices given respectively by

$$M_0 = \iiint_\Omega \Psi\Psi^T dv, \tag{3.8}$$

$$M = (M_{ij}), \quad M_{ij} = \iiint_\Omega \rho_h g_{ij} \Phi\Phi^T dv, \tag{3.9}$$

$$M_1(\rho_h) = \iiint_\Omega C_v \rho_h \Psi\Psi^T dv. \tag{3.10}$$

The stiffness matrixes, $L, K(\mu_v) = (k_{ij})$, can be expressed as

$$L = \iiint_\Omega k \nabla\Psi \cdot \nabla\Psi^T dv, \tag{3.11}$$

$$\begin{aligned} k_{ij}(\mu_v) = \iiint_\Omega \mu_v \Big\{ & (g^{mk} g_{ij} + \delta_j^m \delta_i^k - \frac{2}{3}\sigma_j^m \delta_j^k) \partial_m \Phi \partial_k \Phi^T \\ & + (g_{im} \partial_j g^{mk} - \tfrac{2}{3}\partial_j \ln\sqrt{g}\,\delta_i^k) \partial_k \Phi\Phi^T \\ & + (g^{mk} \partial_i g_{mj} - \tfrac{2}{3}\partial_i \ln\sqrt{g}\,\delta_j^k) \Phi \partial_k \Phi^T \\ & - (\tfrac{1}{2}\partial_j g^{mk} \partial_i g_{mk} + \tfrac{2}{3}\partial_i \ln\sqrt{g}\,\partial_j \ln\sqrt{g}\,\partial_j \ln\sqrt{g}) \Phi\Phi^T \Big\} dv. \end{aligned} \tag{3.12}$$

The nonlinear matrix $N(\rho, W) = (N_{ij})$,

$$\begin{aligned} N_{ij} = \iiint_\Omega -\rho \{ & \frac{1}{2} w^n (g_{ij}\delta_n^m + g_{ni}\delta_j^m) \partial_m \Phi\Phi^T \\ & - (2\varepsilon_{ijk}\omega^k + \tfrac{1}{2}\partial_i g_{mj} w^m) \Phi\Phi^T \} dv. \end{aligned} \tag{3.13}$$

The nonlinear matrix $N_0(\rho, W)$ is

$$N_0(\rho, w) = -\iiint_\Omega C_v \rho w^i \partial_i \Psi\Psi^T dx + \iiint_\Omega (r-1) C_v \rho \ \mathrm{div}\ w \Psi\Psi^T dv. \tag{3.14}$$

In a similar manner, we have

$$\begin{aligned} E(w)\rho &= \iiint_\Omega (\rho \partial_j w^j \Psi + \rho w^j \partial_j \Psi) dv - \iint_\Gamma \rho w n \Psi ds, \\ F &= \iiint_\Omega \{ (r-1) C_v \rho T \partial_i \Phi + ((r-1) C_v \rho T \ \partial_i \ln\sqrt{g} + \omega^2 \rho g_{ij} r^j + g_{ij} f^j) \Phi dv \\ &\quad + \iint_\Gamma (\tau^{kj} - \rho w^k w^j) n_j g_{ki} \Phi dv, \\ F_0 &= \iiint_\Omega (f_e + h) \Psi dv + \iint_\Gamma (k \frac{\partial T}{\partial n} - T \rho w n) \Psi ds. \end{aligned}$$

4. Time Discretization and the Splitting Method

Let $u^T = \{\rho, T, w^1, w^2, w^3\}$. Then the dynamic system of Eqs. (4.1)–(4.3) can be expressed in the form of

$$\frac{du}{dt} + A(u) = f, \qquad u(0) = u_0 \tag{4.1}$$

where A is an operator from the Hilbert space H into H. Let A_1 and A_2 be two operators such that

$$A(u) = A_1(u) + A_2(u) \tag{4.2}$$

with $\Delta t(\Delta t > 0)$ as a time discretization step. We consider the splitting method by taking advantage of decomposition. Let θ belong to the open interval (0, 0.5). The idea is to split the time interval $[n\Delta t, (n+1)\Delta t]$ into three subintervals, and integrate for the time interval $[n\Delta t, (n+\theta)\Delta t]$ with an implicit scheme for A_1 and an explicit scheme for A_2. Then, switch the role of A_1 and A_2 for intervals $[(n+\theta)\Delta t, (n+1-\theta)\Delta t]$ and $[(n+1-\theta)\Delta t, (n+1)\Delta t]$. Following these steps, we obtain for each step

$$\begin{aligned}
&\frac{u^{n+\theta}-u^n}{\theta\Delta t}+A_1(u^{n+\theta})+A_2(u^n)=f^{n+\theta},\\
&\frac{u^{n+1-\theta}-u^{n+\theta}}{(1-2\theta)\Delta t}+A_1(u^{n+\theta})+A_2(u^{n+1-\theta})=f^{n+1-\theta},\\
&\frac{u^{n+1}-u^{m+1-\theta}}{\theta\Delta t}+A_1(u^{n+1})+A_2(u^{n+1-\theta})=f^{n+1-\theta},
\end{aligned} \tag{4.3}$$

and u changes from u^n to u^{n+1} through $u^n \to u^{n+\theta} \to u^{n+1-\theta} \to u^{n+1}$. Let

$$\Delta\rho_1=\rho^{n+\theta}-\rho^n,\ \ \Delta\rho_2=\rho^{n+1}-\rho^{n+\theta},\ \ \Delta T_1=T^{n+\theta}-T^n,\ \ \Delta T_2=T^{n+1}-T^{n+\theta},$$
$$\Delta W^{(1)}=W^{n+\theta}-W^n,\ \ \Delta W^{(2)}=W^{n+1-\theta}-W^{n+\theta},\ \ \Delta W^{(3)}=W^{n+1}-W^{n+1-\theta}.$$

Application of Eq. (4.3) to the aerodynamic system of Eps. (3.5)–(3.7) leads to

Step 1.

$$\begin{aligned}
&\frac{1}{\theta\Delta t}M_0\Delta\rho_1+\alpha E(W^n)\Delta\rho_1=-E(W^n)\rho^n,\\
&\frac{1}{\theta\Delta t}M(\rho^n)\Delta W^{(1)}+\alpha K(\mu_v^n)\Delta W^{(1)}=F(\rho^n,T^n)-K(\mu_v^n)W^n-N(\rho^n,W^n)W^n\\
&\frac{1}{\theta\Delta t}M_1(\rho^n)\Delta T_1+\alpha L\Delta T_1=F_0(W^n)-LT^n-N_0(\rho^n,W^n)T^n.
\end{aligned} \tag{4.4}$$

Step 2.

$$\begin{aligned}
&\frac{1}{(1-2\theta)\Delta t}M(\rho^{n+\theta})\Delta W^{(2)}+\beta K(\mu_v^{n+\theta})\Delta W^{(2)}+N(\rho^{n+\theta},W^{n+\theta}\\
&+\Delta W^{(2)})\Delta W^{(2)}+N(\rho^{n+\theta},W^{n+\theta}+\Delta W^{(2)})W^{n+\theta}\\
&=F(\rho^{n+\theta},T^{n+\theta})-K(\mu_v^{n+\theta})W^{n+\theta}.
\end{aligned} \tag{4.5}$$

Step 3.

$$\begin{aligned}
&\frac{1}{\theta\Delta t}M_0\Delta\rho_2+\alpha E(W^{n+1-\theta})\Delta\rho_2=E(W^{n+1-\theta})\rho^{n+\theta},\\
&\frac{1}{\theta\Delta t}M(\rho^{n+\theta})\Delta W^{(3)}+\alpha K(\mu_v^{n+1-\theta})\Delta W^{(3)}\\
&=F(\rho^{n+\theta},T^{n+\theta}),-K(\mu_v^{n+1-\theta})W^{n+1-\theta}-N(\rho^{n+\theta},W^{n+1-\theta})W^{n+1-\theta},\\
&\frac{1}{\theta\Delta t}M_1(\rho^{n+\theta})\Delta T_2+\alpha L\Delta T_2=F_0(W^{n+1-\theta})-LT^{n+\theta}-N_0(\rho^{n+\theta},W^{n+1-\theta})T^{n+\theta}.
\end{aligned} \tag{4.6}$$

We use two kinds of element: 27–node isoparameter element for velocity; and 8–node isoparameter element for density, temperature and pressure.

In addition, the adaptive method and the (p, h) variation method by Babuska may be employed. The mesh will be refined or the order of the element will be raised according to accuracy in the elements. The finite element grid generation is carried out automatically.

It is obvious that splitting leads to linear and nonlinear algebraic systems. An efficacious algorithm for the linear system will be employed, while the optimal control method will be used to solve the nonlinear subproblems.

5. Numerical Experiment

Figure 1 shows the computational grid for a projectile. Figures 1a and 1b show the longitudinal cross section and circumferential distribution of the computational grid, respectively. This element has 19 in the streamwise direction, 14 in the circumferential direction and in 21 the normal direction.

The flow over the projectile at 4^0 angle of attack and the Reynolds number 5×10^6 based on the model length was computed. The mode used for the computational study presented here is an idealization of a real artillery projectile geometry. Figures 2 and 3 show the surface pressure distribution in the lee side and wind side, respectively. The experimental data are from [1] and [2].

References

[1] L. D. Kayser, K. Whiton, Surface Pressure Measurements on a Boattailed Projectile Shape at Transonic Speeds, US Army Ballistic Research Laboratory, ARBRL –MR– 03161, March 1982.

[2] L. D. Kayser, Base Pressure Measurements on a Projectile Shape at Mach Numbers from 0.91 to 1.20, US Army Ballistic Research Laboratory, ARBRL –MR– 03353, April 1984.

[3] M. O. Bristeau, R. Glowinski, J. Periaux, Numerical Methods for the Navier-Stokes Equations and Applications to the simulation of Compressible and Incompressible Viscous Flows, Research Report UH / MD–4, February 1987.

[4] T. J. Coakley, Turbulence Modeling Methods for the Compressible Navier-Stokes Equations, AIAA 16th Fluid and Plasma Dynamics Conference, July 12–14, 1983.

[5] W. B. Sturk, D. C. Mylin, Computational Parametric Study of the Magnus Effect on Boattailed Shell at Supersonic Speeds, AIAA Paper No.81–1900, 8th Atmospheric Flight Mechanics Conference, August 1981.

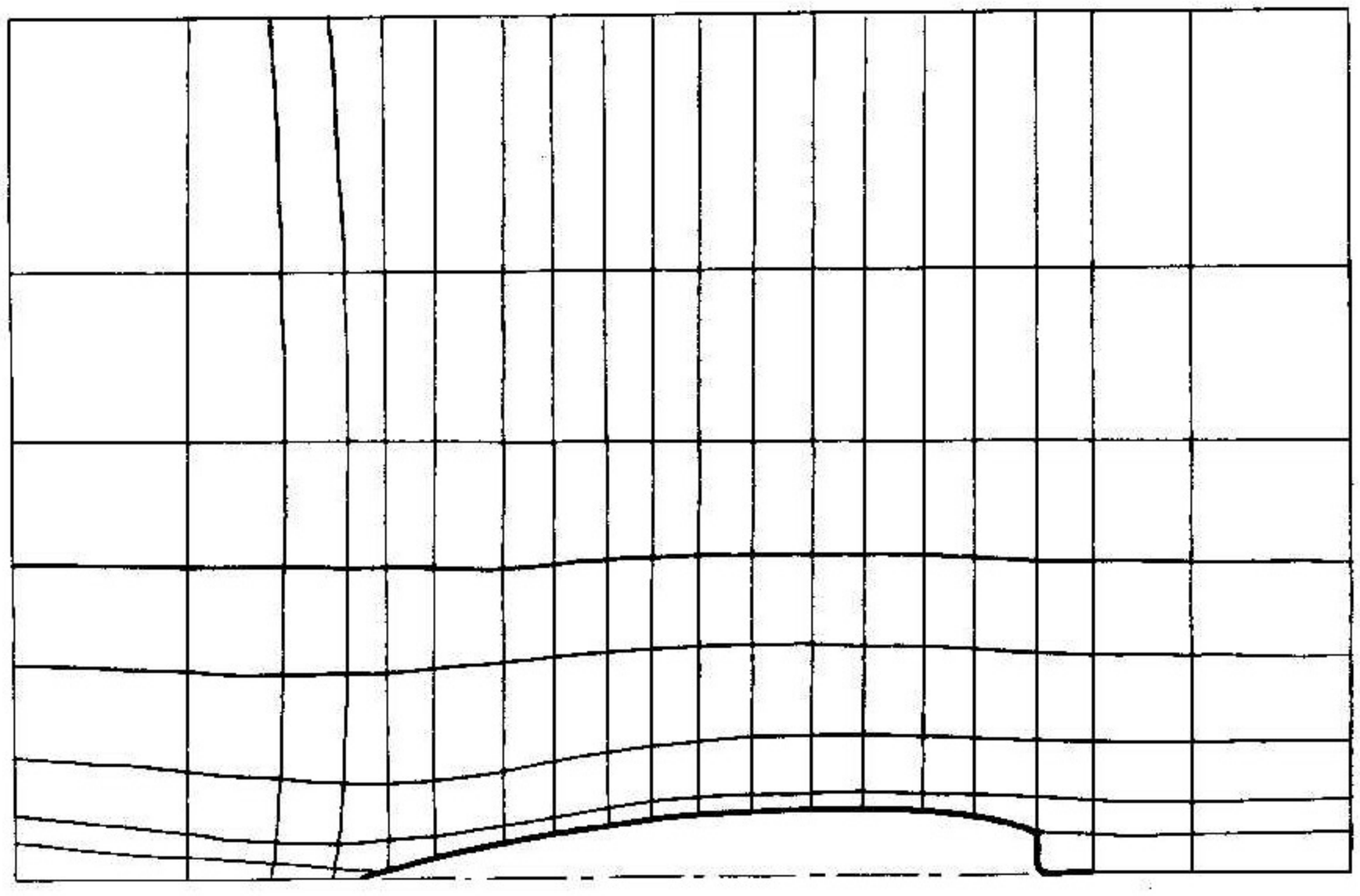

Figure 1a. Computational Grid (Longitudinal Cross Section).

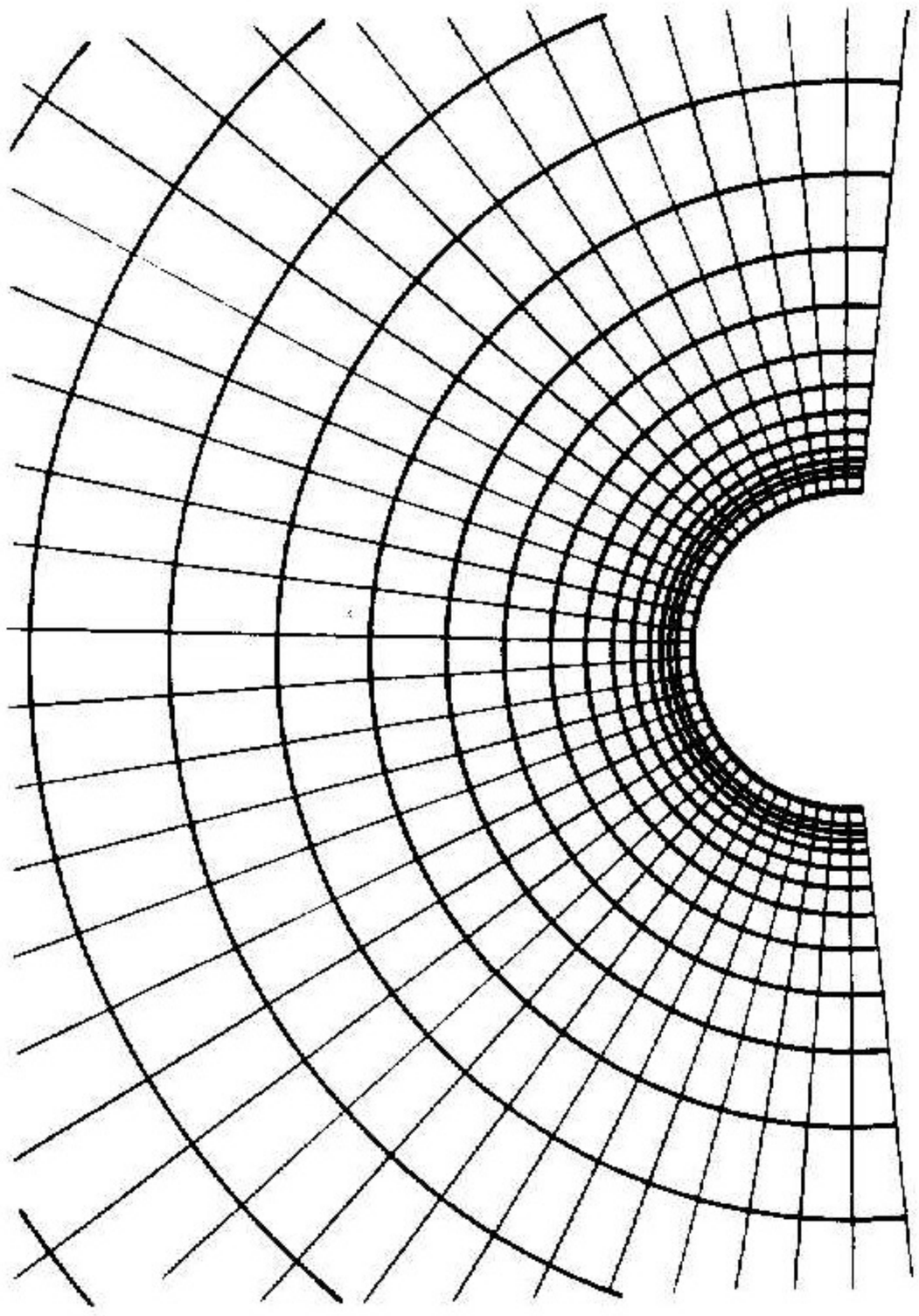

Figure 1b. Computational Grid (Circumferential Distribution)

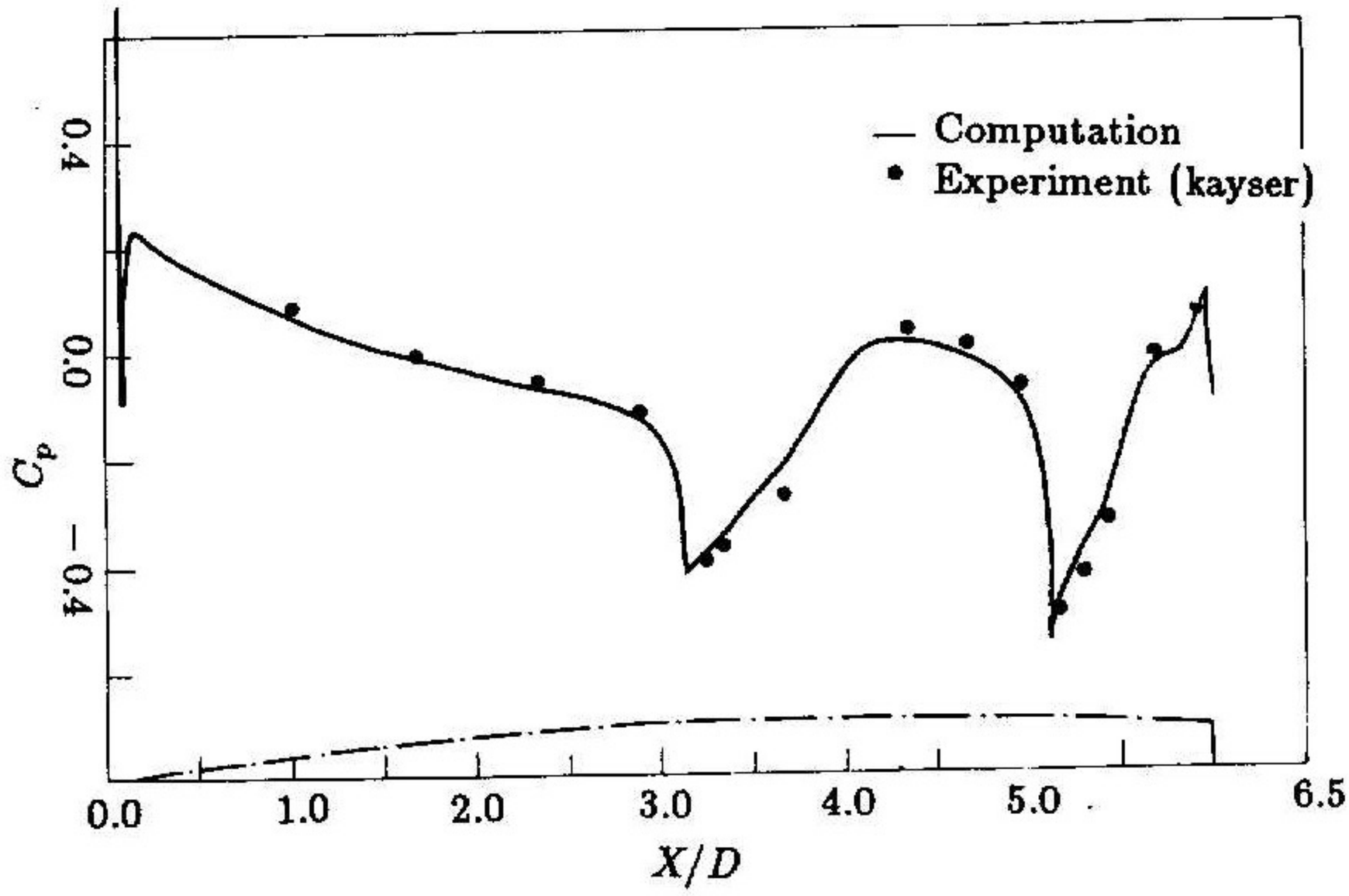

Figure 2. Longitudinal Surface Pressure Distribution, Lee Side, $M_\infty = 0.96$ and $\alpha = 4^0$

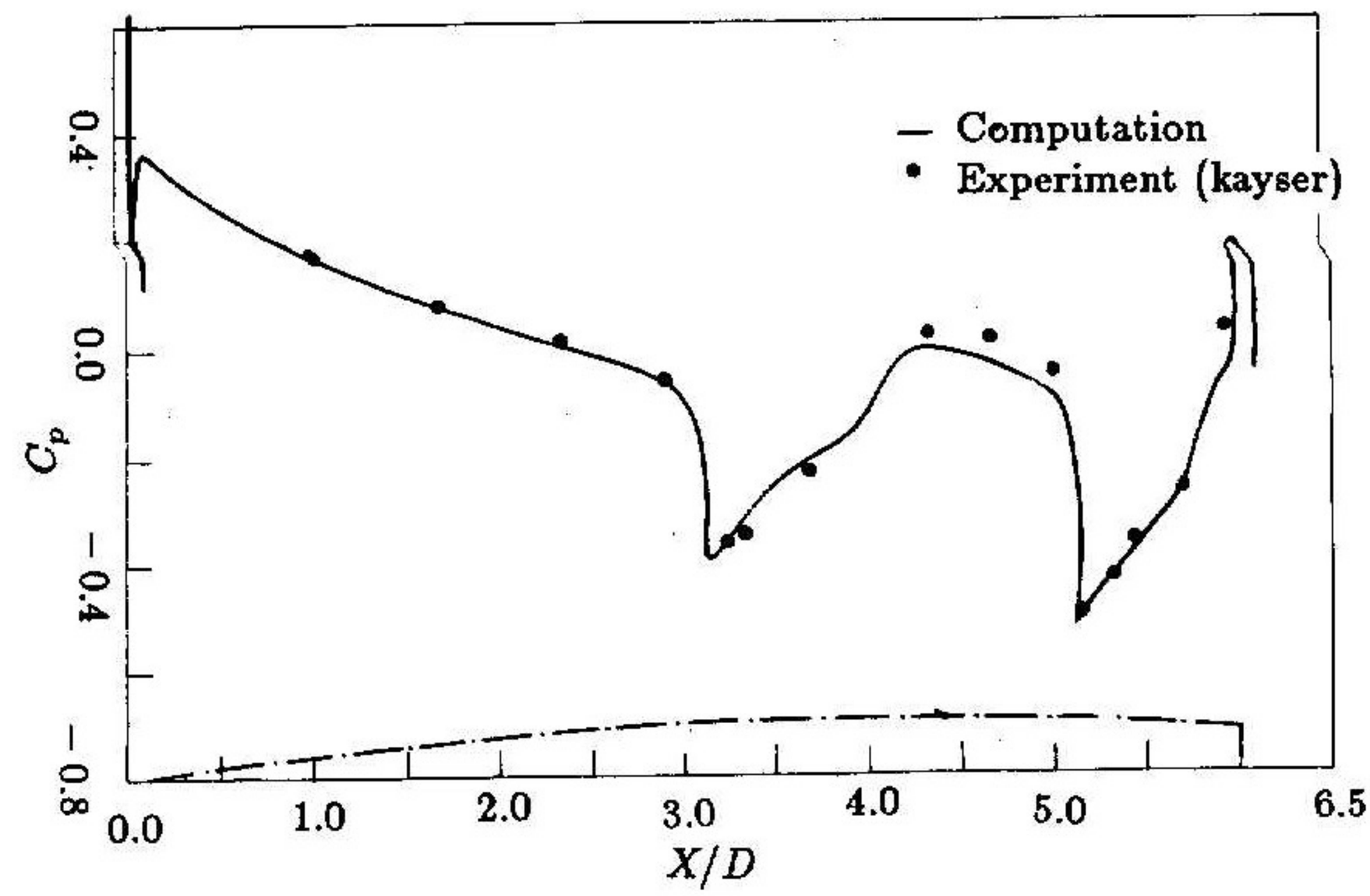

Figure 3. Longitudinal Surface Pressure Distrbution, Wind Side $M_\infty = 0.96$ and $\alpha = 4^0$